Hindawi
Wireless Communications and Mobile Computing
Volume 2022, Article ID 6585189, 13 pages
https://doi.org/10.1155/2022/6585189

Research Article

Detection and Function of Elastic Wave Tomography of Foundation Piles of High-Rise Buildings under the Background of Internet of Things

Wannan Guo[1] **and Yang Liu**[2]

[1]*School of Mechanics and Engineering, Liaoning Technical University, Fuxin, 123000 Liaoning, China*
[2]*School of Management, Dalian Polytechnic University, Dalian, 116034 Liaoning, China*

Correspondence should be addressed to Yang Liu; 20071120200726@xy.dlpu.edu.cn

Received 28 April 2022; Revised 23 June 2022; Accepted 4 July 2022; Published 25 July 2022

Academic Editor: Jun Ye

Foundation piles are a widely used foundation form for high-rise buildings. Its main function is to reduce the settlement of buildings. In recent years, in areas with good upper soil conditions, in order to reduce the amount of earthwork excavation and transportation, more and more engineering buildings use foundation piles. Therefore, the status of foundation piles in construction projects is becoming more and more important. The high-rise building foundation pile project belongs to the underground concealed project. In the construction process, it is greatly affected by factors such as construction technology and geology. After the construction is completed, it is difficult to observe the changes inside the foundation pile with the naked eye as time goes by. A series of problems such as building collapse, settlement, and cracking often occur, thus affecting normal use and causing some safety accidents. In order to solve these series of problems, this paper proposes an elastic wave tomography detection method. It performs imaging inversion calculation on the inside of the foundation pile, and many methods are used in it. In the canonical Gaussian-damped Newton method in tomography, its iteration rate is 3.5% higher than that of the canonical Gaussian-Newton method, the convergence speed is accelerated, the accuracy is high, and the error is small. In the process of detection, this method is more suitable to detect the integrity and quality of foundation piles.

1. Introduction

Elastic wave tomography technology is a computer detection system based on the Internet of Things. It involves many subjects such as mathematics, physics, computer, engineering, and materials and has a wide range of application value. Tomography is also called computer-aided tomography. It is a reconstruction technique from data to image. It can reflect the internal quality of the tested material or workpiece through pseudocolor images and conduct qualitative and quantitative analysis of defects, thereby improving the reliability of detection. Due to the misjudgment or design error of the bearing capacity of the foundation by the exploration unit, a series of problems such as building collapse, shortening of service life, construction quality, cutting corners, and incomplete foundation pouring are caused. This brings security risks to the project. The detection of building foundation piles has been paid more and more attention. In this paper, elastic wave tomography technology is used to detect the interior of high-rise building foundation piles, and the elastic wave equation model, cross-hole CT observation system, tomography forward, and inversion methods are used. The purpose is to detect the bearing capacity of the foundation pile and the integrity of the pile body and analyze the defects of the pile body.

Elastic wave tomography can quickly and effectively determine the physical and mechanical properties of rock or concrete. Using the computer imaging results of the Internet of Things, the acoustic parameters are accurately given to determine the stability of the building foundation piles.

It lays the foundation for the comprehensive detection of foundation piles of high-rise foundation buildings from single strength measurement to crack measurement, defect measurement, damage layer thickness measurement, and elastic parameter measurement.

China classifies residential buildings with more than 10 floors and other civil and industrial buildings with a height of more than 24 meters as high-rise buildings. Generally, the service life of high-rise buildings is about 70 years. After decades of load-bearing use, the foundation piles of buildings undergo uneven deformation, uneven settlement, or inclination over time. This leads to loose and aged pile structures, cracks, fractures, and collapses, causing a series of safety problems. In response to this set of issues, Asaue et al. performed preventive and proactive maintenance on in-service concrete slabs to determine civil engineering forecasts. To determine the maintenance system based on the predictions of the concrete slabs, they evaluated the evolution of fatigue damage and internal defects. They research and develop acoustic emission (AE) tomography and elastic wave tomography as innovative nondestructive testing (NDT) methods for the detection of concrete quality. The three-dimensional velocity distribution within the panel is determined by the method described above, and damaged or degraded areas are identified. The results show good agreement between the predicted low-velocity region and the damage region estimated from crack distribution, displacement, and strain. At locations where cracks are strongly observed, the velocity drops below 3400 m/s. In addition, regions with velocities below 2700 m/s were also observed in slabs reaching the fatigue limit [1]. According to photoacoustic computed tomography (PACT) technology, Mitsuhashi et al. used optical contrast and ultrasonic detection principles to form images of photoacoustic-induced initial pressure distribution in tissues to detect internal damage of high-rise building foundation piles. The PACT reconstruction problem corresponds to an inverse source problem, where the initial pressure distribution is recovered from measurements of the radiated wavefield. When ultrasonic waves propagate in a medium, absorption, scattering, and mode conversion from longitudinal to transverse waves occur. In this paper, a forward model based on time-domain finite-difference discretization of the three-dimensional elastic wave equation is established, and the corresponding adjoint calculation method of the forward operator is given. A large scale of these operators employing multiple graphics processing units has also been developed and implemented [2]. Huang et al. investigated the dynamical effective parameters and crack arrest behavior of multidegree-of-freedom locally resonant metamaterials. Based on the Wiener-Hopf method, the energy release rate, which characterizes the crack splitting resistance, is deduced, and the influence of material parameters is discussed. Compared with single-atom lattice chains and locally resonant metamaterials composed of single-degree-of-freedom unit cells, this new multidegree-of-freedom-coupled periodic structure exhibits some fundamental features during crack propagation. The results show that the dynamic crack propagation in elastic wave metamaterials exhibits a lower energy release rate due to the coupling of different displacements. This shows that it has better fracture resistance and crack arrest properties. This work is expected to provide a way to improve the crack growth resistance of advanced materials and structures [3]. He et al. proposed a new elastic wave metamaterial. It consists of vertical and lateral resonators and orthogonal stiffeners. An active feedback control system is used to extend the tunable range in the low and high frequency regions and to change the acoustic structure coupling characteristics. The effective mass density under different feedback constants is discussed. To reflect the effect of fluid-solid interactions, they considered immersing elastic wave metamaterials in different fluid media and calculated their acoustic transmission loss (STL). This work provides a feasible method for building mechanical/acoustic models with multifunctional potentials [4].

Depending on the form or material of the foundation piles, there may be an unacceptable decrease in the foundation bearing capacity of buildings and structures under construction. To control the quality of cast-in-place reinforced concrete piles, based on the analysis of the excited and recorded elastic wave parameters in the piles, Lozovsky et al. combined ultrasonic monitoring of concrete integrity using sensors in access pipes installed in reinforced cages. Numerical simulations of the propagation of elastic waves are carried out. Their research was carried out on a series of 2D bored pile models. These bored piles had no defects, but had soil inclusions, or access pipes and concrete debonding. The possibilities and limitations of this method are summarized. The location and geometry of the defect, as well as the influence of the adhesion failure of the access pipe and concrete on the measurement results, are demonstrated. It requires additional studies of abnormal wellbore tomography before drawing conclusions about the possibility and further using the pile as part of the foundation. General recommendations are given regarding the number of access pipes arranged in the pile and the selection of the time interval for calculating the attenuation. Their results show that it is incorrect to calculate the strength of the pile material by the speed of wave propagation [5]. Cui et al. used the finite element software ABAQUS to simulate the process of detecting piles by ultrasonic transmission method. The influence of the inclined acoustic tube on the test results of foundation piles is analyzed. The results show that after the pile is completed, due to the inclination of the sound tube, the sound depth curve velocity of the received signal is inclined to one side, and the sound velocity deviates seriously from the normal value. When the pile body has defects, due to the inclination of the acoustic tube, the defect signal is not obvious, and it is easy to miss or misjudge the pile body defect. In order to solve the problem of tilting the sound tube, a mathematical model of the positional relationship of the sound tube is established, and the sound velocity correction method based on the angle of the sound tube is deduced. Validation showed that the corrected acoustic signal was able to accurately determine the defect and its location in the pile. This effectively reduces the influence of the inclined sound tube on the detection signal, which is beneficial to improve the accuracy of the detection of the pile body [6].

The realization of tomography has two basic processes: forward and inversion. For forward inversion research, Espinosa et al. used the full waveform inversion (FWI) method to solve the inverse problem, imaging high acoustic impedance contrast experimental data of different test targets. The method is based on a high-resolution numerical simulation of the wave-medium interaction forward problem, considering the full time series. To reduce the complexity of numerical implementation, the model takes into account fluid media. Therefore, they aimed to evaluate the accuracy of reconstruction under this assumption for materials with varying degrees of shear wave attenuation and to investigate the limitations of this assumption. The sound velocity images obtained with experimental data are given, and the reconstruction accuracy is evaluated. Their future work should include viscoelastic materials [7]. The above studies on elastic waves, tomography, and forward and inversion are in-depth and have reference significance for this article.

Elastic wave tomography is a new type of geophysical method, mainly used for nondestructive testing of concrete structures. In this paper, the elastic wave tomography detection method is used to perform tomography detection on the foundation piles of high-rise buildings. It combines ultrasonic detection technology, cross-hole CT observation system, and tomography forward and inversion technology to perform inversion imaging analysis on the inner medium of high-rise building foundation piles. In this way, the quality of foundation piles can be evaluated, and some potential safety hazards caused by damage to foundation piles can be avoided.

2. Detection Method of Foundation Pile Elastic Wave Tomography

Tomography technology is based on ray scanning, inversion calculation of the obtained information. It reconstructs the image of the distribution law of the elastic wave and electromagnetic wave parameters of the rock mass within the measured range, to achieve a geophysical inversion interpretation method for delineating the geological anomaly. Elastic wave tomography is one of the classification of tomography techniques and is often used in the detection of building foundation piles [8]. Elastic wave tomography has the characteristics of high exploration accuracy, good reliability, intuitive and clear images, small site requirements, and strong anti-interference ability [9].

2.1. Elastic Wave Tomography Detection

(1) Imaging principle of elastic wave tomography and elastic wave equation model

The elastic wave tomography detection technology mainly uses an Internet of Things detection system. The dry ray beam formed by the propagation of elastic waves in different media forms a tangent surface of the object during the detection process. Then, according to the parameter changes of the wave-initial signal on the cut plane, discrete image reconstruction is performed in the Internet of Things computer to generate an internal image of the object. It goes on to infer the technology of the internal physical properties and states of objects [10]. As shown in Figure 1, it is a schematic diagram of fan-shaped wave ray projection detected by elastic wave tomography. First, the elastic wave is used to detect from the outside of the object, and the projection data is obtained. Finally, the data is overlapped in small blocks, the internal image of the object is quantified, and then, the internal information of the object is reconstructed. When an elastic wave penetrates a medium, the speed of the wave is related to the integrity, density, elastic modulus, and shear modulus of the medium. In the application of nondestructive testing of concrete structures, the higher the density, the higher the strength, and the better the integrity of the detected object, the faster the elastic wave propagates and the smaller the attenuation. If the detected object is broken loose, not vibrated tightly, and the strength is low, the elastic wave will not only reduce the transmitted wave speed but also attenuate rapidly.

The elastic wave displacement equation of motion can be obtained from the imaging principle:

$$(\alpha + \beta)\nabla(\nabla \cdot w) + \beta\nabla^2 w + \wedge = \rho\ddot{w}. \tag{1}$$

When $\wedge = 0$, in a small medium, if the compressive deformation and volume expansion change are ignored, and only the rotational or shear deformation inside the medium is considered, then the case of no scattered field displacement is expressed by the equation:

$$\nabla \cdot w = 0. \tag{2}$$

Substituting the equation for free-field displacement into the equation yields:

$$\nabla^2 w = \frac{\rho}{\beta}\ddot{w} = \frac{\ddot{w}}{c_e^2}. \tag{3}$$

When the medium is in a uniform state, the propagation velocity of the shear wave can be obtained by the following equation:

$$c_e^2 = \frac{\rho}{\beta}. \tag{4}$$

When the curl of the medium displacement is equal to 0, it represents the position change of the particle, which is a directed line segment from the initial position to the final position. Its size has nothing to do with the path, and the direction is from the start point to the end point. It is a physical quantity with magnitude and direction, that is, a vector.

It can get:

$$\nabla \times w = 0. \tag{5}$$

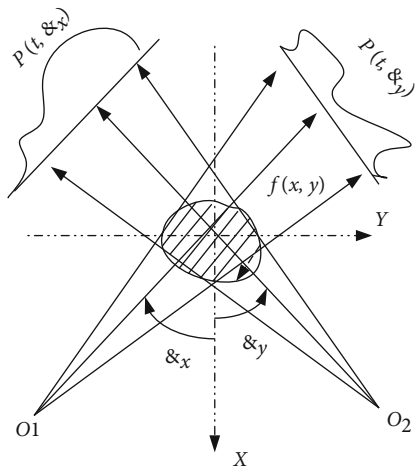

Figure 1: Schematic diagram of fan-wave ray projection for elastic wave tomography detection.

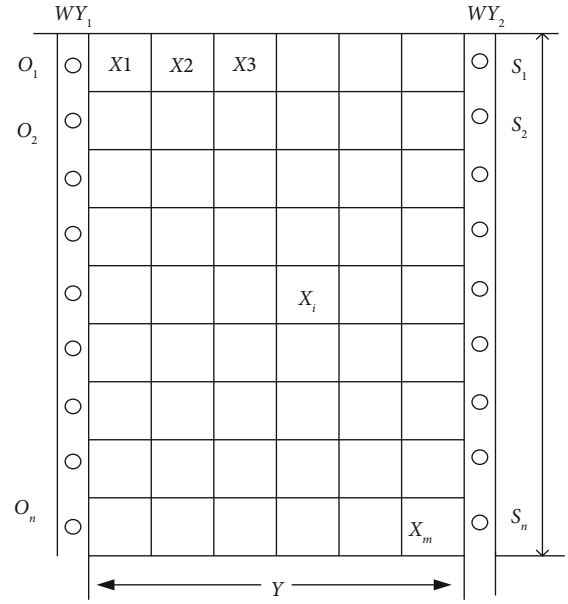

Figure 2: The layout of borehole CT measurement.

Also because:

$$\nabla^2 = \nabla(\nabla \cdot w) - \nabla \times \nabla \times w = \nabla(\nabla \cdot w). \tag{6}$$

Substituting the above equation into the elastic wave displacement equation of motion, it can get:

$$\nabla^2 w = \frac{\rho}{\partial + 2\beta} \ddot{w} = \frac{\ddot{w}}{c_R^2} c_R^2 = \frac{\partial + 2\beta}{\rho}. \tag{7}$$

This is the elastic wave equation for expansion and contraction waves. When the curl of displacement is 0, under the premise of no rotational deformation, when the unit inside the elastic medium expands, deforms, or compresses, the elastic mass only reciprocates at the position centered on the equilibrium position. Its motion direction is consistent with the propagation direction of elastic waves [11]. Among them, the displacement is a vector, and the landmark is a scalar. Displacement is the straight-line distance from the start point to the end point, and the distance is the length of the path.

2.2. Cross-Bore CT Observation System. The cross-hole CT observation system is to perform tomography of transmitted waves between two drilled plates. The cross-hole CT observation system is often used for high-precision interhole formation imaging detection. In the first hole, the transmitter transmits the transmitted wave and reaches the second hole and is received by the detector. The data is transmitted to the transmission recorder for postprocessing analysis, and the transmitted wave propagation paths are superimposed and then imaged, as shown in Figure 2. WY_1 is the excitation hole, and a row of excitation points is arranged along the excitation hole. WY_2 is the receiving hole, and the row next to the receiving hole is the receiving point.

First, the section between the excitation hole and the receiving hole is divided into several squares of equal area, and the space of the forming area is discretized. Assuming that the number of squares in the horizontal space is y, and the number of squares in the vertical space is l, then the total number of squares is $f = y \times l$. The size of the square can be determined according to the size of the object to be detected and the amount of data.

Assuming the inverse of the wave velocity of the jth square, the ray equation for each ray wave can be obtained:

$$u_1 w_1 + u_2 w_2 + \cdots + u_m w_m = f_1, \tag{8}$$

$$\sum_{j=1}^{m} u_j w_j = f_i, i = 1, 2, \cdots, n. \tag{9}$$

Among them, f_i is the arrival time of the wave during the propagation of the ith ray, and u_j is the length of the i th ray in the jth square.

If the depths of the excitation of the two boreholes are different during the measurement process, and x times are received, X-ray equations can be obtained. The matrix equation for the resulting ray travel time equation is:

$$\begin{bmatrix} u_{11} u_{12} \cdots u_{1m} \\ u_{21} u_{22} \cdots u_{2m} \\ \cdots\cdots\cdots\cdots \\ u_{x1} u_{x2} \cdots u_{xm} \end{bmatrix} \begin{bmatrix} u_1 \\ u_2 \\ \cdots \\ u_m \end{bmatrix} = \begin{bmatrix} f_1 \\ f_2 \\ \cdots \\ f_x \end{bmatrix}. \tag{10}$$

The above equation can be abbreviated as:

$$AU = f. \tag{11}$$

The size of x and m depends on the number of rays. When solving this system of equations, the wave slowness

values within the squares give the result. Then, take the reciprocal value to get the distribution diagram of the wave velocity value between holes.

2.3. Acoustic Detection Method. The line source of elastic wave tomography detection technology is elastic wave [12]. In elastic wave detection, the most commonly used emission waves are ultrasonic waves and seismic waves, of which ultrasonic waves are one of the most commonly used methods for engineering detection [13]. The difference between elastic waves and ultrasonic waves: the energy of elastic waves is greater than that of ultrasonic waves, and ultrasonic waves decay quickly. The propagation speed of elastic waves in the medium is relatively stable, while the speed of ultrasonic waves is relatively high. One excitation point in elastic waves can form multiple rays. The speed of the elastic wave when passing through the medium reflects the integrity and density of the medium. Acoustic tomography technology obtains information by penetrating the medium and inverts the imaging through the Internet of Things computer. Finally, the sound wave velocity distribution map of the medium is obtained to judge the quality of the medium [14]. Ultrasonic testing has the characteristics of high precision and accurate positioning of abnormal points and is one of the most commonly used defect detection methods. As shown in Figure 3, it is the process of ultrasonic testing.

There are many types of transducers for ultrasonic testing of concrete, such as flat type (high frequency), Langevin type (low frequency), radial supercharged type, and one-shot double-received type. According to the different positions of the ultrasonic transducer in the foundation pile, ultrasonic detection can be divided into three different ways. The first is the ultrasonic transmission method in the foundation pile. The second is the ultrasonic transmission method outside the foundation pile. Both methods are single-hole transmission, as shown in Figure 4. The third is the transhole transmission method in the pile, as shown in Figure 5.

Ultrasonic testing mainly judges the quality of the medium through the wave speed. The elastic properties of concrete itself enable ultrasonic waves to reflect the compositional relationship of their internal structures when propagating in concrete. Generally speaking, the greater the speed of sound within a certain range, the greater the strength of the concrete, and the quality of the concrete can be guaranteed. The smaller the speed of sound, the lower the concrete strength, and the quality of the concrete of the pile body is defective. If the area with low speed of sound is large and the measuring points are continuous, it will bring security risks to the use of the project [15]. Therefore, the ultrasonic sound velocity plays an important role in judging the quality of foundation piles.

Taking the foundation piles of high-rise buildings as the detection object, the foundation piles of general buildings are completed with concrete pouring. In the sound velocity evaluation, for the foundation piles with good quality, the fluctuation state of the sound velocity is consistent with the fluctuation of the concrete quality, and both obey the normal distribution [16]. In practice, the method often used to analyze the speed of sound is the probabilistic method. Another method is the lower limit value method of sound speed. When the critical value of the abnormal sound speed is too small, the probability method cannot judge the defect. The basic principle of the probability method is to judge the quality of the foundation pile by whether the sound velocity generated by the ultrasonic wave in the concrete foundation pile obeys the normal distribution law.

It arranges the sound velocity of any profile survey point in order of largest to smallest:

$$s_1 \geq s_2 \geq \cdots s_i \geq \cdots s_{p-k} \geq \cdots s_{p-1} \geq s_p. \tag{12}$$

Among them, i represents the sound velocity measurement value of the ith measuring point; p is the number of measurement points on the value plane; k refers to the number of the smallest value in the final sequence.

The equation for the statistical calculation value:

$$s_0 = s_e - \partial_{Fs}, \tag{13}$$

$$s_e = \frac{1}{p - k\sum_{i=1}^{p-k} s_i}, \tag{14}$$

$$W_s = \sqrt{\frac{1}{p-k-1}\sum_{i=1}^{p-k}(s_i - s_e)^2}. \tag{15}$$

Among them, s_0 is the judgment value for criticizing the abnormality of the medium; s_e is the average of the number of (p-k); W_s is the standard deviation of the number of (p-k); ∂ is the corresponding number of (p-k).

The basic principle of the PSD criterion is that the measured sound on any section is continuously derivable with the change of the height of the measuring point. When the concrete has defects, the relationship between the two is discontinuous and nonderivative [17]. This criterion discards the assumption that the acoustic time values are normally distributed. It is based on the mutation of the properties of the ultrasonic propagation medium at the defect. The variation law of the defect area of the acoustic time value is a discontinuous function. The equation expression of the PSD criterion is:

$$F_i = \frac{(y_i - y_{i-1})^2}{(k_i - k_{i-1})}. \tag{16}$$

Among them, y_i, y_{i-1} represents the acoustic time value between two adjacent measurement points, and k_i, k_{i-1} represents the depth value between two adjacent measurement points. Practice has proved that the PSD criterion is very sensitive to defects, and the time-to-acoustic changes caused by nondefect factors are all gradual processes [18].

The most commonly used waveforms for ultrasonic nondestructive testing are shear wave and longitudinal wave [19]. The propagation speed of transverse waves

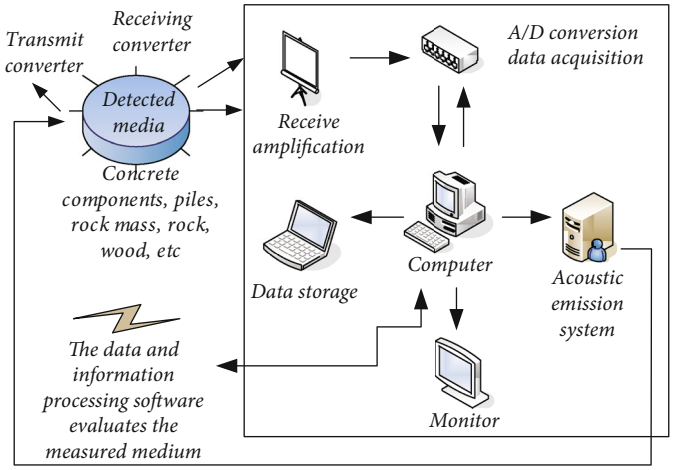

Figure 3: Ultrasonic testing process diagram.

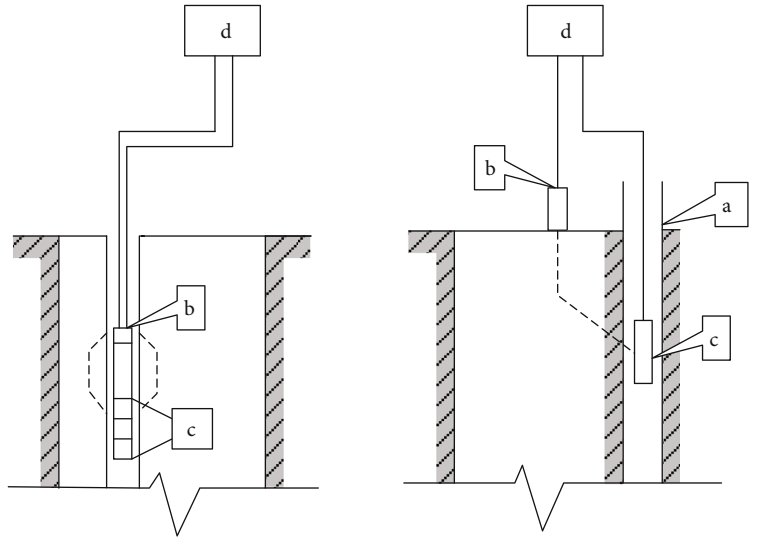

Figure 4: Ultrasonic transmission method inside and outside the foundation pile.

and longitudinal waves are different, and the particle will cause the superposition of the two vibrations, and then, the conversion of vibration modes will occur. Surface waves whose amplitude decays as they go deeper into the surface appear at the free interface of a solid. The propagation of sound waves in bounded solids also produces guided waves, which are waves with more complex vibrations. The difference between longitudinal waves and transverse waves is that the former is a wave with parallel propagation directions, and is a propelling wave, which is less destructive. The latter is a wave whose propagation direction is vertical, and is a shear wave, which is more destructive.

(1) The longitudinal wave velocity of an infinite body, expressed by the elastic constant:

$$d_g = \sqrt{\frac{F(1-\beta)}{\rho(1+\beta)(1-2\beta)}}. \tag{17}$$

Among them, F represents the elastic modulus; $\beta < 0.5$ represents Poisson's ratio, dimensionless; ρ refers to the density of the medium.

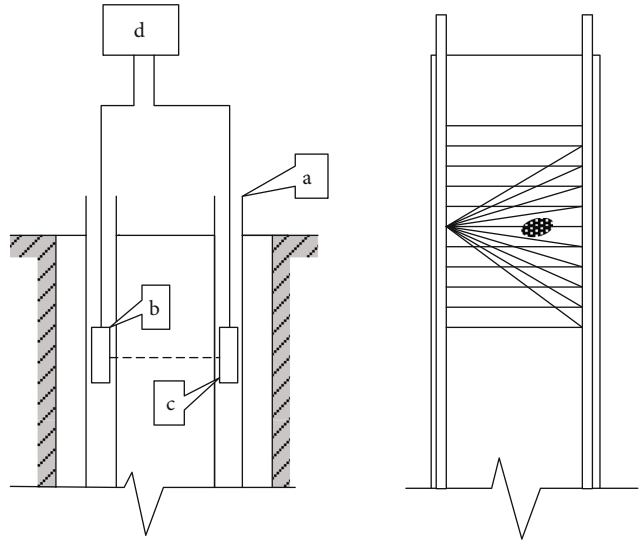

a. Acoustic tube
b. Transmitting transducer
c. Receiving transducer
d. Ultrasonic detector

Figure 5: Schematic diagram of cross-hole transmission method in foundation pile.

(2) Infinite bulk shear wave velocity, expressed by elastic constant

$$d_p = \sqrt{\frac{S}{\rho}} = \sqrt{\frac{F}{2\rho(1+\beta)}}. \tag{18}$$

In the equation, S represents shear modulus; other parameters are the same as above.

(3) The ratio of longitudinal wave velocity to shear wave velocity

$$\frac{d_g}{d_p} = \sqrt{\frac{2(1-\beta)}{(1-2\beta)}}. \tag{19}$$

In the equation, when $\beta = 0.25$, $d_g/d_p = \sqrt{3} = 1.7321$. The β of concrete is between 0.2 and 0.25, and the β of dense rock is 0.25, so it can be seen that the sound speed of transverse waves is smaller than that of longitudinal waves.

(4) The surface wave velocity of an infinite body, expressed by the elastic constant:

$$d_R = \frac{0.87 + 1.12\alpha}{1+\beta}\sqrt{\frac{S}{\rho}} = \frac{0.87 + 1.12\beta}{1+\beta} d_p. \tag{20}$$

2.4. Tomographic Forward and Inversion. The realization of tomography has two basic processes: forward and inversion. There is a certain energy relationship between forward and inversion. Forward modeling is the basis for full waveform inversion. The inversion imaging results are related to the forward calculation results [20]. Figure 6 is the staggered grid of forward calculation.

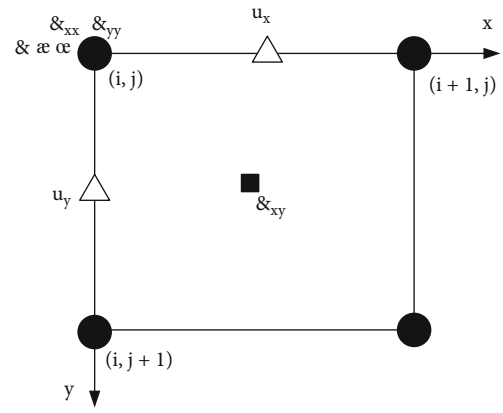

Figure 6: Staggered grid for forward calculation.

Forward modeling is the analysis basis for the three major links of acoustic wave data acquisition, data processing, and interpretation evaluation and is the basis for inversion calculation. Forward modeling assumes the simulated structure of the acoustic wave propagation medium. On this basis, according to the physical law of sound wave propagation, the sound wave data information obtained at the sound wave receiving place is predicted, that is, the sound wave record [21]. Forward modeling has the following functions: first, it provides a theoretical basis for the acquisition and processing of acoustic data and can evaluate the scientificity and feasibility of the method. The second is to detect the authenticity of the results and the accuracy of the inversion algorithm.

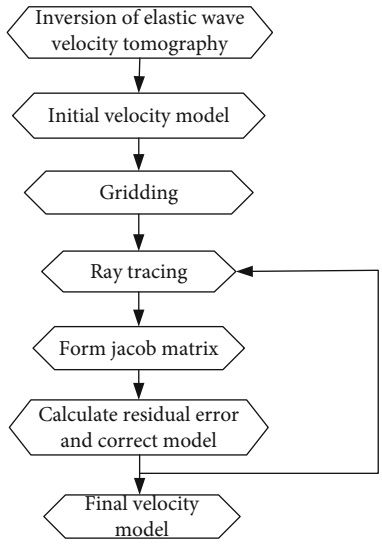

Figure 7: Flow chart of elastic wave tomography inversion calculation

Table 1: List of detection parameters.

Stake number	Survey line	Interval of measuring points (m)	Test pile length (m)
1	AB	0.5	30.4
	BC	0.5	30.4
	AC	0.5	30.6
2	AB	0.5	36.0
	BC	0.5	36.0
	AC	0.5	36.0
3	AB	0.5	36.0
	BC	0.5	36.0
	AC	0.5	36.0
4	AB	0.5	46.0
	BC	0.5	46.5
	AC	0.5	46.0
5	AB	0.5	46.5
	BC	0.5	46.5
	AC	0.5	46.5

Through the canonical Gauss-Newton method and forward calculation, it can obtain the observation return $w = k(m)$ about the acoustic wave and the medium eucalyptus, where w is the data information and m is the model information [22]. K are generalized mapping operators, which represent the relationship between the model and the data. The inversion calculation is to obtain the parameters of the model by solving the observation equation, that is, the velocity model. The most suitable velocity model can be directly found through the observation equation calculated by the forward calculation. This makes the final observation data the closest to the real data, finding the minimum value of the objective function [23]. In this paper, statistical theory is used to calculate the inversion problem. To sum up in principle, the tomography can be interpreted with the following inversion algorithm steps, as shown in Figure 7.

Table 2: Summary of test results.

Stake number	Survey line	Pile evaluation and defect location	Comprehensive evaluation
1#	AB	Complete	I
	BC	Complete	
	AC	Complete	
2#	AB	Complete	I
	BC	Complete	
	AC	Complete	
3#	AB	26.5 m defective	III
	BC	Complete	
	AC	25.5 m, 26.5 m defective	
4#	AB	Complete	I
	BC	Complete	
	AC	Complete	
5#	AB	Complete	I
	BC	Complete	
	AC	Complete	

(1) Regular Gauss-Newton method for statistical inversion

Derivative for any component, it can get:

$$\frac{\alpha L_\beta(T)}{\alpha T_q} = \frac{2}{G}\sum_{p=1}^{G}\frac{\alpha A(T)_p}{\alpha T_q}\left[A(T)_p - \widehat{F}_p\right] + \lambda\frac{2}{K}\sum_{q=1}^{K}\left[T_q - Y\left(T_q\right)\right]. \tag{21}$$

The gradient in the equation yields:

$$\nabla L_\beta(T) = \frac{2}{G}\nabla A(T)^R\left[A(T) - \widehat{F}\right] + \beta\frac{2}{G}\left[T - Y(T)\right]. \tag{22}$$

The Hesse matrix of the objective function is:

$$\nabla^2 L_\beta(T) = \frac{2}{G}\nabla A(T)^R\nabla A(T) + \beta\frac{2}{G}I_{M\times M}. \tag{23}$$

(2) Regular Gauss-damped Newton method for statistical inversion

In the iterative equation of the regular Gauss-Newton method, in order to speed up the iterative convergence process, it is determined whether the Hesse matrix is positive

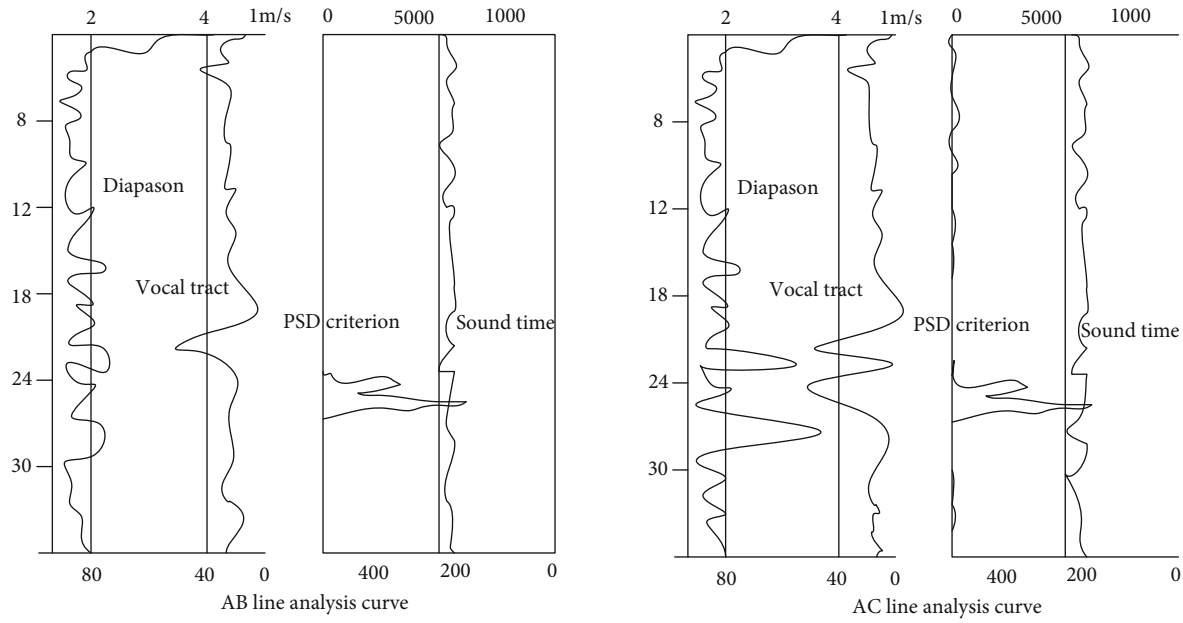

Figure 8: Analysis curve of AB survey line and AC survey line in no. 3 foundation pile.

Table 3: Profile inspection data.

	Sound velocity (km/s)	Amplitude (dB)	Sound time (μs)	PSD (μs^2/m)	Frequency (kHz)
Maximum	5.09	104.6	228	5780	49.019
Minimum value	3.728	73.3	167	0	19.607
Average value	4.614	97.85	185.7	121.03	37.523
Standard deviation	0.189	4.71	9.5		3.832
Deviation	4.10%	4.81%	5.10%		10.21%

definite. Given the regularization parameter $\beta \geq 1$, compute the process gradient:

$$\nabla^2 L_\beta\left(T^{(l)}\right) = \frac{2}{G}\nabla A\left(T^{(l)}\right)^R \nabla A\left(T^{(l)}\right) + \beta\frac{2}{G} I_{M\times M}. \quad (24)$$

Newtonian directions are calculated:

$$g^{(l)} = -\left[\nabla^2 L\left(T^{(l)}\right)\right]^{-1} \nabla L\left(T^{(l)}\right). \quad (25)$$

2.5. Role of Elastic Wave Tomography Detection

(1) As a method of engineering quality detection, elastic wave layer imaging technology is more convenient and simple, with high detection accuracy, light instrument, high work efficiency, and fast image reconstruction and analysis. It can accurately detect the defects of high-rise building foundation piles, and the detection effect is good [24]

(2) Elastic wave tomography detection can quantitatively give the distribution map of physical property parameters inside the medium. The physical and mechanical properties of rock or concrete can be determined quickly and efficiently. According to the imaging results, the acoustic parameters are accurately given to determine the stability of the building foundation piles, which brings convenience to the internal detection activities

3. Experiment on Elastic Wave Tomography of Foundation Piles of High-Rise Buildings

3.1. Effectiveness of Elastic Wave Tomography Detection on Foundation Piles. The pile foundation has good performance such as high bearing capacity, small settlement, and can withstand a certain level and uplift force. It is widely used in bridge engineering, deep-sea and shallow-sea oil production platforms, and special soils such as frozen soil and expansive soil. The basic task of an ultrasonic detector for concrete quality testing is to emit ultrasonic pulse waves to the tested concrete. At the other end of the concrete, the sound wave is received by the receiving transducer, and the sound signal is converted into an electrical signal. After the data acquisition is completed, it is automatically displayed

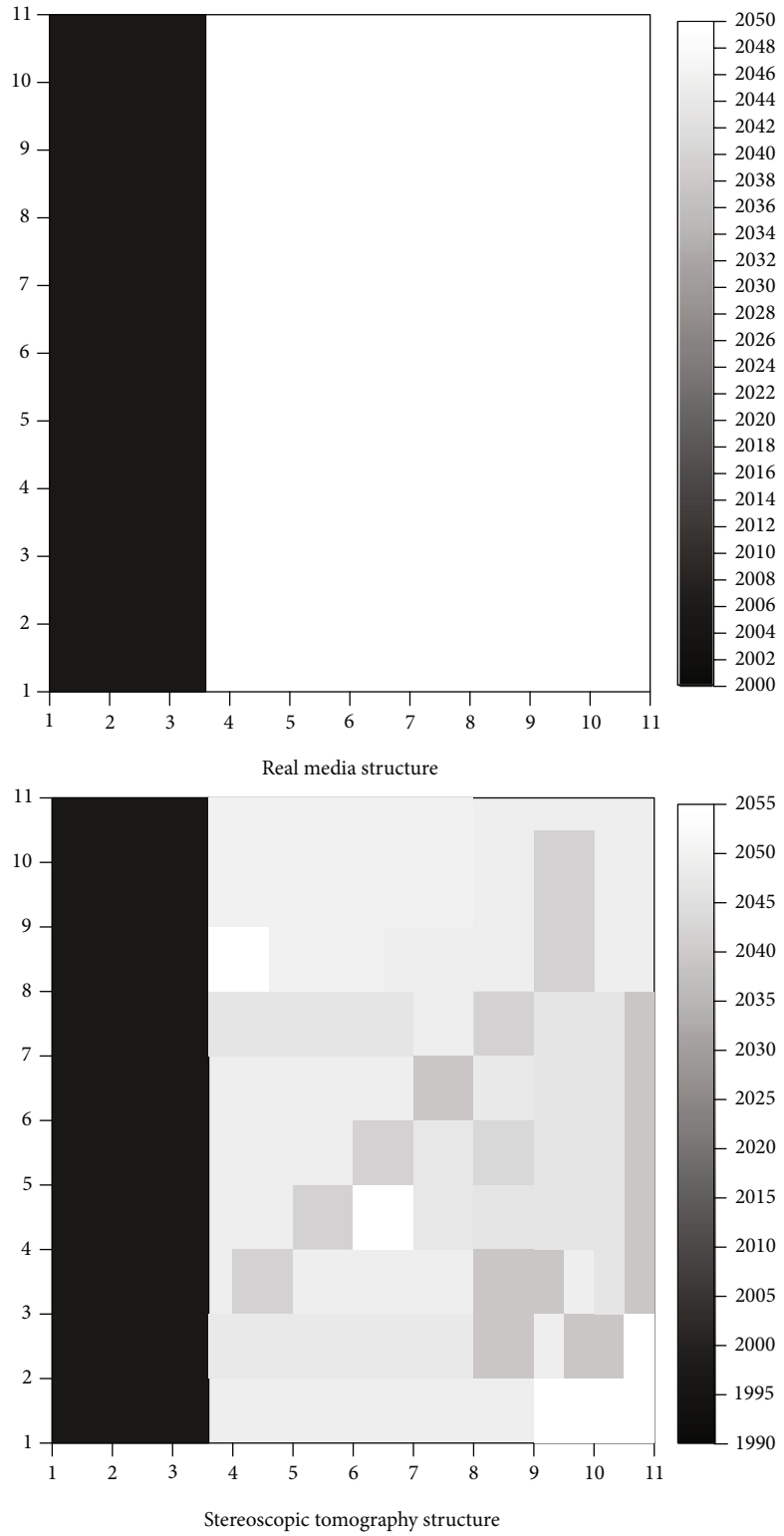

Figure 9: Real-medium structure diagram and stereo tomography results.

on the display after being processed and calculated by the software, and the data is stored in the storage system at the same time. Taking the high-rise building foundation pile as an example for tomographic analysis, the diameter of the high foundation pile is 800 mm. It is assumed that the length of the foundation pile is 11.8 m, which is made of general concrete, and the bearing layer at the bottom of the foundation pile is strongly weathered sandstone. The test depth of

Table 4: Inversion calculation workload of medium model parameters.

Numerical simulation and algorithm		Number of iterations (times)	CPU time consuming (points)	$\frac{V - V^*}{V^*}$
Numerical simulation 1	Algorithm 4.1	60	36.835	0.021332
	Algorithm 4.2	54	34.186	0.040343
	Algorithm 4.3	35	29.211	0.050868
Numerical simulation 2	Algorithm 4.1	62	34.797	0.020848
	Algorithm 4.2	52	33.940	0.025816
	Algorithm 4.3	34	29.176	0.055962

elastic wave in the experiment is -9~-13.25 m. The integrity of the foundation piles of the project is tested by ultrasonic projection method to judge the quality of the project. According to the algorithm, it is judged whether there are defects such as fracture and subsidence. For example, Table 1 is a preview of the detection parameters, and Table 2 is the detection results of all foundation piles.

The results show that, in the no. 3 foundation pile, the positions of the main defects detected in the two survey lines AB and AC are at 26.5 m of AB, 25.5 m, and 26.5 m of AC. Other pile bodies have no defects found so far. It shows that the quality of most of the pile bodies is relatively good. Figure 8 is the analysis curve of the AB survey line and the AC survey line in the no. 3 foundation pile.

It can be seen from the analysis of the imaging curve that the sound speed and the wave amplitude are greater than the critical value of the sound speed and the wave amplitude, indicating that the internal condition of the foundation pile is good, and the quality of the concrete is relatively good. However, during the detection process of the sub-3 piles, the sound velocity and wave amplitude near 25~26 m fluctuated greatly and decreased at the same time, which was lower than the normal critical value. This indicates that the pile at this location is defective. In the same pile, AC imaging of piles between 25 and 26 m also showed that the detected sound velocity and amplitude were lower than normal critical values. The curve of acoustic parameters and depth of profile shows abnormal changes of PSD parameters at AB and AC. The speed of sound changes. After analysis, these two points are measured values at discontinuous intervals, and the speed of sound is greater than the critical value of the speed of sound. Defects are therefore detected. Combined with the above survey line analysis curve, the detection data of the profile can be obtained, as shown in Table 3.

The parameters such as sound time, sound speed, sound amplitude, and frequency of concrete at other survey lines are normal. The dispersion is 5.10%, 4.10%, 4.81%, and 10.21%. It can be judged that there is no defect in the internal structure. When there is a defect in the concrete, since the speed of sound of impurities such as soil and air in the defect area is much lower than that of the sound concrete, the transit time increases significantly, and the sound time value also increases accordingly. It can be seen that the acoustic time value is an important parameter for judging whether there is a defect in the concrete. During the inspection of the no. 3 pile, the acoustic parameters at 25-26 m changed significantly, so another judgment was made that there was a defect inside the no. 3 pile.

3.2. Tomographic Forward and Inversion Experiments. Taking the foundation piles of high-rise buildings as the experimental object, the inversion simulation is carried out by the regular Gauss-Newton method of statistical inversion in the two foundation piles, and two simulation graphs are obtained. According to the nonlinear least squares method, the velocity model is updated, and the step factor is searched. Although the velocity model is updated, it is necessary to ensure that the value of the objective function does not change. It iterates the velocity model once, and then goes through multiple inversion iterations. This makes little change in the velocity model, and the final result of the volume tomographic image after iteration can be obtained.

Figure 9 shows the real medium structure diagram and the stereo tomography results. The velocity model is established by model meshing. When the y-axis coordinate is greater than or equal to 100, the velocity value is 2050. The velocity value of the y-axis coordinate less than 100 is 2000, and the initial velocity value is set to 1900. According to the above inversion iteration results, the relative error between the inversion result and the exact value is obtained, as shown in Table 4.

As can be seen from the table, the canonical Gauss-damped Newton method for statistical inversion tends to converge faster. In Algorithm 3, the number of iterations is only 35, the time spent is 29.211, and the number of iterations is less. And each iteration takes less time on average, so it speeds up the iterative process. But the relative error between the inversion result and the exact value can be seen that the relative error of using the regular Gauss-Newton method is small. During simulation 1 and simulation 2, the iteration time of the regular Gauss-damped Newton method is about 3.5% faster than that of the regular Gauss-Newton method, and the iteration rate is increased. Therefore, in the case of less knowledge of the background experience of the inversion, it can be seen from the simulation effect that the regular Gauss-damped Newton method is more suitable. Therefore, it is not difficult to see from the previous theoretical derivation and numerical test results that these algorithms are all effective algorithms for inversion calculation of medium model parameters and demonstrate the efficiency and practicability of the algorithms.

4. Discussion

In this paper, the principle of elastic wave tomography is introduced first. Then, the elastic wave equation model is introduced, and some technical method principles are extended from elastic waves. In the experimental part, elastic wave tomography technology and ultrasonic technology are used to detect the damage of high-rise building foundation piles. The method is applied to the actual operation process, and the role of these methods is expounded. From elastic wave tomography and distribution, inversion and forward modeling are carried out through experiments to obtain experimental data. The experimental results show that the elastic wave tomography technology plays an important role in detecting whether the foundation piles of high-rise buildings are defective.

5. Conclusions

This paper focuses on the detection process and role of elastic wave tomography in high-rise building inspection in the context of the Internet of Things. The defects and damages of high-rise buildings are analyzed from four major perspectives: elastic wave, cross-hole CT observation system, acoustic wave defect detection, and tomography forward and inversion. Based on the applicability and function of detection, the computer imaging is analyzed. It judges whether the internal medium is damaged from parameters such as sound time, sound speed, sound amplitude, and frequency, thereby improving the safety of foundation piles. This effectively solves the influence of construction technology, geology, and other factors during the construction process. After the construction is completed, a series of building collapses, settlements, and cracks will affect the normal use of foundation piles and cause some safety accidents over time. However, during the experiment, many problems were encountered, and the experimental data was not comprehensive enough, so it looked forward to future research to have better solutions.

Data Availability

The data that support the findings of this study are available from the corresponding author upon reasonable request.

Conflicts of Interest

The authors declare that they have no conflicts of interest.

References

[1] T. Asaue, T. Nishida, T. Maeshima et al., "Evolution of fatigue damage in wheel-loading tests evaluated by 3D elastic-wave tomography," *Journal of Disaster Research*, vol. 12, no. 3, pp. 487–495, 2017.

[2] K. Mitsuhashi, J. Poudel, T. P. Matthews, A. Garcia-Uribe, L. V. Wang, and M. A. Anastasio, "A forward-adjoint operator pair based on the elastic wave equation for use in transcranial photoacoustic computed tomography," *SIAM Journal on Imaging Sciences*, vol. 10, no. 4, pp. 2022–2048, 2017.

[3] K. X. Huang, G. S. Shui, Y. Z. Wang, and Y. S. Wang, "Enhanced fracture resistance induced by coupling multiple degrees of freedom in elastic wave metamaterials with local resonators," *Journal of Elasticity*, vol. 144, no. 1, pp. 33–53, 2021.

[4] Z. H. He, Y. Z. Wang, and Y. S. Wang, "Sound transmission tuned by active feedback control attached to elastic wave metamaterials immersed in water," *Journal of Applied Mechanics*, vol. 88, no. 7, pp. 1–28, 2021.

[5] I. N. Lozovsky, R. A. Zhostkov, and A. A. Churkin, "Numerical simulation of ultrasonic pile integrity testing," *Russian Journal of Nondestructive Testing*, vol. 56, no. 1, pp. 1–11, 2020.

[6] Y. Cui, Z. Ma, Y. Yang, and D. Song, "Acoustic velocity correcting method for the tilted acoustic tube in testing of pile by ultrasonic transmission," *Advances in Civil Engineering*, vol. 2020, Article ID 8824739, 8 pages, 2020.

[7] L. Espinosa, E. Doveri, S. Bernard, V. Monteiller, R. Guillermin, and P. Lasaygues, "Ultrasonic imaging of high-contrasted objects based on full-waveform inversion: limits under fluid modeling," *Ultrasonic Imaging*, vol. 43, no. 2, pp. 88–99, 2021.

[8] L. Yi, L. Sun, X. Ming, and M. Zou, "Full-depth spectral domain optical coherence tomography technology insensitive to phase disturbance," *Biomedical Optics Express*, vol. 9, no. 10, pp. 5071–5083, 2018.

[9] A. L. Perchuk and A. A. Serdyuk, "Phase relations in spinel Lherzolite KLB-1 according to results of thermodynamic modeling up to 30 GPa: peculiarities of mineral assemblages and geodynamic effects," *Petrology*, vol. 30, no. 2, pp. 198–211, 2022.

[10] J. Xie, M. H. Ritzwoller, and S. J. Brownlee, "Inferring the oriented elastic tensor from surface wave observations: preliminary application across the western United States," *Geophysical Journal International*, vol. 201, no. 2, pp. 996–1021, 2015.

[11] J. Li, Z. Feng, and S. Gerard, "Wave-equation dispersion inversion," *Geophysical Journal International*, vol. 208, no. 3, pp. 1567–1578, 2017.

[12] R. Grzeszick, A. Plinge, and G. A. Fink, "Bag-of-features methods for acoustic event detection and classification," *IEEE/ACM Transactions on Audio Speech & Language Processing*, vol. 25, no. 6, pp. 1242–1252, 2017.

[13] D. Vangi, M. Bruzzi, and J. N. Caron, "Compact probe for non-contact ultrasonic inspection with the gas-coupled laser acoustic detection (GCLAD) technique," *Experimental Mechanics*, vol. 62, no. 3, pp. 403–415, 2022.

[14] B. Zheng, J. Zhang, and T. Feng, "Large deformation mechanics of gob-side roadway and its controlling methods in deep coal mining: a case study," *Advances in Civil Engineering*, vol. 2020, Article ID 8887088, 13 pages, 2020.

[15] M. Song and W. Zhu, "Elastic wave propagation in strongly nonlinear lattices and its active control," *Journal of Applied Mechanics*, vol. 88, no. 7, pp. 1–25, 2021.

[16] Z. Li, Y. Wang, and Y. Wang, "Tunable three-dimensional nonreciprocal transmission in a layered nonlinear elastic wave metamaterial by initial stresses," *Applied Mathematics and Mechanics*, vol. 43, no. 2, pp. 167–184, 2022.

[17] N. P. Aleshin, A. A. Kirillov, and L. Y. Mogilner, "A general solution of the problem of elastic-wave scattering by a plane crack," *Doklady Physics*, vol. 66, no. 7, pp. 202–208, 2021.

[18] X. Yang, Z. Li, and H. Liu, "Using refined theory to studied elastic wave scattering and dynamic stress concentrations in plates with two cutouts," *Journal of Applied Mathematics and Physics*, vol. 8, no. 12, pp. 2999–3018, 2020.

[19] G. Sha, "Attenuation and phase velocity of elastic wave in textured polycrystals with ellipsoidal grains of arbitrary crystal symmetry," *Acoustics*, vol. 2, no. 1, pp. 51–72, 2020.

[20] N. U. Kuldoshov, N. R. Kulmuratov, and M. R. Ishmamatov, "Numerical solution of the problem of the action of a plane unsteady elastic wave on cylindrical bodies," *Theoretical & Applied Science*, vol. 91, no. 11, pp. 352–360, 2020.

[21] Z. Li, H. Liu, and W. Zhen, "Elastic wave scattering and dynamic stress concentrations around double holes in piezoelectric media," *Journal of Applied Mathematics and Physics*, vol. 8, no. 12, pp. 3060–3069, 2020.

[22] B. Afa and C. Ipab, "A novel method for investigation of acoustic and elastic wave phenomena using numerical experiments," *Theoretical and Applied Mechanics Letters*, vol. 10, no. 5, pp. 307–314, 2020.

[23] S. J. Horning, M. E. Juweid, H. Schöder et al., "Interim positron emission tomography scans in diffuse large B-cell lymphoma: an independent expert nuclear medicine evaluation of the Eastern Cooperative Oncology Group E3404 study," *Blood*, vol. 115, no. 4, pp. 775–777, 2010.

[24] L. Nguyen, "A family of inversion formulas in thermoacoustic tomography," *Inverse Problems & Imaging*, vol. 3, no. 4, pp. 649–675, 2009.